Magnetic Resonance Materials in Physics, Biology and Medicine (2020) 33:283–292
https://doi.org/10.1007/s10334-019-00777-9

RESEARCH ARTICLE

Histogram analysis of apparent diffusion coefficients for predicting pelvic lymph node metastasis in patients with uterine cervical cancer

Jiyeong Lee[1] · Chan Kyo Kim[1,2,3] · Sung Yoon Park[1]

Received: 21 June 2019 / Revised: 29 July 2019 / Accepted: 16 September 2019 / Published online: 23 September 2019

Abstract

Objective To investigate the value of apparent diffusion coefficient (ADC) histogram analysis in predicting pelvic lymph node (LN) metastasis in patients with cervical cancer undergoing surgery.

Materials and methods A total of 162 cervical cancer patients who underwent radical abdominal hysterectomy with pelvic LN dissection performed with pelvic 3 T-MRI including diffusion-weighted imaging were enrolled in this study. The ADC histogram variables (minimum, mean, median, 97.5th percentile [$ADC_{97.5}$], and maximum) of the tumors were developed using in-house software. For predicting pelvic LN metastasis, clinical and imaging variables were evaluated using logistic regression and receiver-operating characteristic (ROC) analyses.

Results Pelvic LN metastasis was identified histopathologically in 50 patients (30.9%). In patients with LN metastasis, all ADC histogram variables were significantly different from those without LN metastasis (all $p < 0.01$). Univariate analysis demonstrated that long- and short-axis diameter of LN, MRI T-stage, squamous cell carcinoma antigen, tumor size, and the $ADC_{97.5}$ were significantly associated with pelvic LN metastasis (all $p < 0.05$). However, multivariate analysis demonstrated that the $ADC_{97.5}$ was the only independent predictor of pelvic LN metastasis (odds ratio, 0.996; $p = 0.001$). The area under the ROC curve of $ADC_{97.5}$ was 0.782, which was the greatest among all variables. Interobserver agreement of all ADC histogram variables was fair to good.

Discussion The $ADC_{97.5}$ from histogram analysis may be a useful marker for the prediction of pelvic LN metastasis in patients with cervical cancer.

Keywords Magnetic resonance imaging · Diffusion-weighted MRI · Cervical cancer · Lymphatic metastasis

Abbreviations

LN	Lymph node
FIGO	International Federation of Gynecology and Obstetrics
DWI	Diffusion-weighted imaging
ADC	Apparent diffusion coefficient
SCC	Squamous cell carcinoma
THRIVE	T1-weighted high-resolution isotropic volume examination
ROI	Region of interest
$ADC_{97.5}$	97.5th percentile ADC
ADC_{mean}	Mean ADC
ADC_{max}	Maximum ADC
ADC_{min}	Minimum ADC
ADC_{median}	Median ADC
ICC	Intraclass correlation coefficient

✉ Chan Kyo Kim
chankyokim@skku.edu

[1] Department of Radiology and Center for Imaging Science, Samsung Medical Center, Sungkyunkwan University School of Medicine, 81 Irwon-ro, Gangnam-gu, Seoul 06351, Republic of Korea

[2] Department of Medical Device Management and Research, SAIHST, Sungkyunkwan University, Seoul, Republic of Korea

[3] Department of Digital Health, SAIHST, Sungkyunkwan University, Seoul, Republic of Korea

Introduction

Uterine cervical cancer is one of the most common cancers in women and continues to be the fourth most common malignancy worldwide [1]. Pelvic or paraaortic lymph node (LN) metastasis is an important prognostic factor for cervical cancer and affects treatment strategies. The presence of LN metastasis is included as stage IIIC classification in the

recent revised clinical staging of the International Federation of Gynecology and Obstetrics (FIGO) [2–4]. Therefore, the detection of preoperative LN metastasis is a crucial issue for patient counseling for determining optimal management and predicting patient prognosis.

Typically, LN metastasis identified by magnetic resonance imaging (MRI) can be evaluated by size or morphologic criteria. The specificity of LN metastasis in cervical cancer is excellent in early-stage cervical cancer, but sensitivity is limited due to the inability to detect normal-sized or normal-shaped LN [5]. Recently, although diffusion-weighted imaging (DWI) has demonstrated a potential for detecting metastatic pelvic LN in gynecological cancer [6, 7], its accuracy in detecting small normal-sized LN metastases is still limited as conventional MRI.

In cervical cancer, DWI is a useful technique for differentiation of pathological subtypes or tumor grade differentiation [6, 8, 9]. In particular, DWI as imaging biomarker has demonstrated the potential for preoperative prediction of therapeutic response, prediction of early therapeutic response, or evaluation of post-treatment survivals [10–13]. To date, however, few studies have reported results of pretreatment DWI in predicting LN metastasis in cervical cancer [14]. Before initiating patient treatments, it would be very important in clinical practice to evaluate whether a tumor has already the likelihood of LN metastasis; LN metastasis is an important prognostic factor. The purpose of this study was to retrospectively investigate the value of apparent diffusion coefficient (ADC) histogram analysis derived from DWI for the prediction of pelvic LN metastasis in patients with cervical cancer.

Methods

Patients

This study protocol was in accordance with the ethical standards of the institutional research committee and with the 1964 Helsinki Declaration. All patients offered written informed consent for MRI examinations. Retrospective analysis was approved by our institutional review board (SMC 2018-11-107). Between April 2011 and September 2013, 175 consecutive patients with biopsy-proven cervical cancer received radical abdominal hysterectomy and pelvic LN dissection with or without paraaortic LN dissection at our institution. Inclusion criteria for patients were: (1) had a routine pelvic 3 T-MRI including DWI ($b = 0$ and 1000 mm^2/s) at our institution before surgery, (2) had not previously undergone radiotherapy or chemotherapy, and (3) were without presence of two or more primary malignancies. Of these, 13 patients were excluded: preoperative concurrent chemoradiotherapy ($n = 9$), double primary malignancies (colon cancer and endometrial cancer, respectively) ($n = 2$), and poor image quality ($n = 2$). Thus, 162 patients (mean age 47.7 years; range 26−81 years) were enrolled in this study (Fig. 1). All clinical data including age, serum squamous cell carcinoma (SCC) antigen, and pathologic outcomes were retrospectively obtained from medical records. The clinical stages of cervical cancers were determined using the FIGO classification [15].

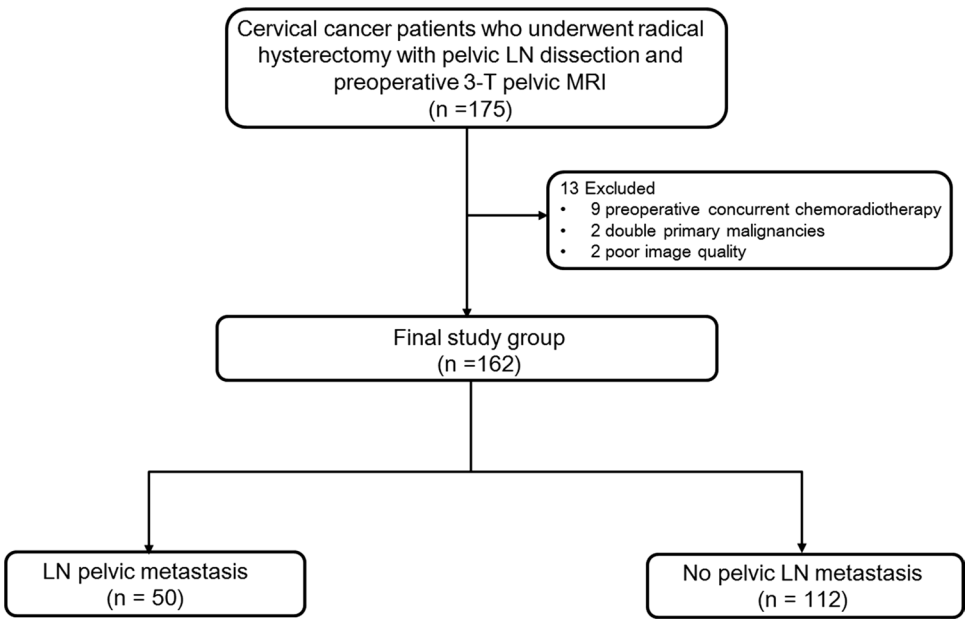

Fig. 1 Flowchart for patient enrollment

MRI protocols

All patients underwent preoperative pelvic MRI using a 3-T MR scanner (Intera Achieva 3.0 TX; Philips Healthcare, Best, The Netherlands) with a phased-array body coil. The MRI protocol included T1-weighted imaging, T2-weighted imaging, DWI and postcontrast fat-saturated T1-weighted High-Resolution Isotropic Volume Examination (THRIVE). T2-weighted turbo spin-echo images (repetition time/echo time, 4568–5320/100 ms; slice thickness, 4 mm; interslice gap, 0.4 mm; matrix, 800 × 690; number of signals acquired (NSA), 3; sensitivity encoding (SENSE) factor, 3; field of view (FOV), 36 cm; and acquisition time, 3 min 30 s) were acquired in three orthogonal planes (axial, sagittal and coronal). Axial T1-weighted turbo spin-echo images were obtained using the following parameters: slice thickness, 5 mm; interslice gap, 2 mm; FOV, 25 cm; number of slices, 26; and acquisition time, 2 min 23 s. Axial DWI was obtained using a short T1 inversion recovery single-shot echo-planar imaging technique with background suppression. Imaging parameters were as the followings: repetition time/echo time, 8000/56 ms; matrix, 128 × 108; slice thickness, 5 mm; interslice gap, 0 mm; NSA, 4; SENSE factor, 2; *b* values, 0 and 1000 s/mm^2; FOV, 35 cm; and acquisition time, 4 min 30 s. ADC maps were automatically constructed using the manufacturer's software and ADC value was calculated with Gaussian monoexponential fit of signal intensity using $b = 0$ and 1000 s/mm^2. Postcontrast fat-saturated THRIVE imaging was acquired in the axial plane (repetition time/echo time = 3.5/1.7 ms, slice thickness = 3–4 mm, interslice gap = 1.5–2 mm, and FOV = 32 cm) at 3 min after a bolus injection of gadolinium contrast (Gadovist, Schering, Germany) at a rate of 3 mL/s with a dose of 0.1 mmol, followed by a flush of 15 mL normal saline.

Image analysis

MR images were analyzed by consensus between two radiologists (CKK and SYP, with 13 years and 4 years of experience in gynecological MRI, respectively) on our picture archiving and communication system (Centricity, GE Heathcare) without any information about the clinical and pathological findings. However, the radiologists were aware that enrolled subjects had a history of biopsy-proven cervical cancer.

Imaging variables of tumor size, long-axis and short-axis diameter of pelvic LN, MRI T-stage, and ADC histogram variables were obtained. Tumor size was defined as the maximum diameter measured on three orthogonal planes of T2-weighted images. After a LN with the greatest diameter in the right and left pelvis (including common iliac, external iliac, internal iliac, and inguinal areas) was separately selected in each patient, long-axis and short-axis diameter of the selected LNs were measured on DWI based on T2-weighted or postcontrast THRIVE images.

DWI data were analyzed using an in-house Matlab-based application (The Mathworks Inc, Natick, MA, USA) on a standard Windows operating system. Values of ADC variables were derived from histogram analysis. Regions of interest (ROIs) were manually drawn around the entire visible tumor on a single-axial ADC map that showed the greatest dimension based on anatomical details of T2-weighted and postcontrast THRIVE images, but it did not include edge voxels to avoid a partial volume effect. The ROIs were selected to exclude cystic or necrotic portion in the tumor (Fig. 2). After the ROIs were determined, the histogram analysis was performed. The ADC variables derived from histogram analysis included mean ADC (ADC_{mean}), maximum ADC (ADC_{max}), minimum ADC (ADC_{min}), median

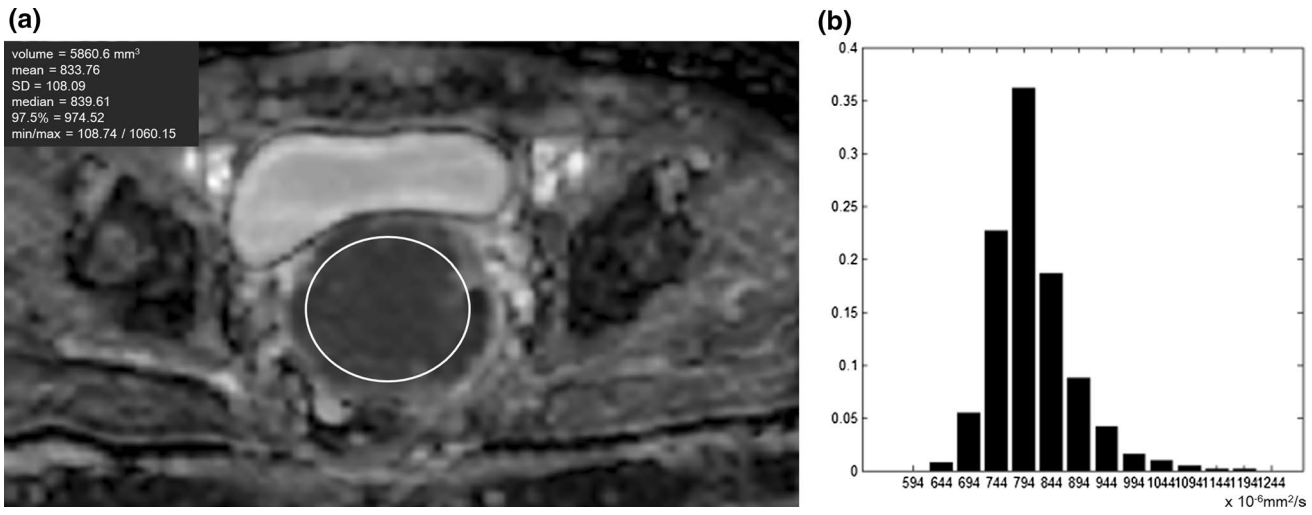

Fig. 2 Method for ADC histogram measurement. **a** Axial ADC map image shows a large cervical tumor of low signal intensity (region-of-interest). **b** ADC histogram of the tumor

ADC (ADC_{median}) and the 97.5th percentile ADC ($ADC_{97.5}$). Additionally, to evaluate interobserver reliability and variability for ADC parameters, a less-experienced radiologist (JL, with 1 year of experience in gynecological MRI) manually drew the ROIs in the tumors for all patients in the same manner as the first measurement.

Statistical analysis

The patients were divided into two groups based on the presence or absence of pelvic LN metastasis on histopathologic findings. Groups were compared to identify differences in age, FIGO stage, SCC antigen level, histologic type, tumor size, long- and short axis-diameter of pelvic LN, MRI T-stage, and ADC variables using independent *t* test, Fisher's exact test, Mann–Whitney test, or Chi square tests.

Univariate and multivariate logistic regression analyses were used to determine whether clinical and imaging variables were associated with pelvic LN metastasis; among ADC variables, we used the $ADC_{97.5}$ which showed the lowest *p* value in descriptive statistics. The variables with *p* value < 0.05 on univariate analysis were further analyzed using multivariate analysis. To evaluate diagnostic performance and identify optimal cutoff values for the prediction of pelvic LN metastasis, receiver-operating characteristic (ROC) curve analysis was used, and the area under the curve (AUC), sensitivity, and specificity were also calculated. Youden index was calculated to identify the optimal cutoff value of each variable for the prediction of pelvic LN metastasis.

Interobserver reliability and variability were evaluated using an intraclass correlation coefficient (ICC) and an Altman–Bland plot, respectively. Reliability suggested by the ICC value was against a scale for poor reliability (0.00–0.20), fair reliability (0.21–0.40), moderate reliability (0.41–0.60), good reliability (0.61–0.80), or excellent reliability (0.81–1.00). A two-sided *p* value < 0.05 was considered statistically significant for all statistical tests. Statistical analyses used SAS software (Version 9.4, SAS institute, Cary, NC).

Results

Basic characteristics

At histopathological findings, pelvic LN metastasis was found in 50 patients (30.9%) and the remaining 112 patients (69.1%) were negative pelvic LN metastasis. Paraaortic LN metastasis was found in seven patients. Characteristics of clinical and imaging variables between patients with and without pelvic LN metastasis are summarized in Table 1. SCC antigen, long-axis and short-axis diameter of pelvic LN, and tumor size were significantly higher in the group with LN metastasis than in the group without LN metastasis (all $p < 0.01$). The group with LN metastasis had significantly higher MRI T-stage than the group without LN metastasis ($p < 0.001$). All ADC variables showed significantly lower values in the group with LN metastasis than in the group without LN metastasis (all $p < 0.01$) (Figs. 3, 4, 5). No significant differences were found between the groups for age, FIGO stage and histologic type (all $p > 0.05$).

Associations between variables and LN metastasis

Table 2 presents the results of logistic regression analyses for predicting pelvic LN metastasis. Univariate analysis demonstrated that long ($p = 0.003$) and short axis ($p < 0.001$) diameter of pelvic LN, MRI T-stage ($p = 0.004$), SCC antigen ($p = 0.044$), tumor size ($p = 0.001$) and $ADC_{97.5}$ ($p < 0.001$) were significantly associated with pelvic LN metastasis. However, multivariate analysis revealed that $ADC_{97.5}$ was the only significant independent predictor (odds ratio = 0.996, $p = 0.001$).

Table 3 presents results of ROC curve analysis for predicting pelvic LN metastasis. The AUC of the $ADC_{97.5}$ was 0.782, which was the greatest among other imaging and clinical variables. With an optimal cutoff value of 1.092×10^{-3} mm^2/s, sensitivity and specificity were 60% and 83%, respectively.

Interobserver reliability and variability

For the interobserver reliability of ADC_{min}, ADC_{mean}, ADC_{median}, $ADC_{97.5}$ and ADC_{max}, ICCs were 0.589 (95% CI 0.458–0.691), 0.712 (95% CI 0.626–0.780), 0.755 (95% CI 0.680–0.814), 0.430 (95% CI 0.228–0.583) and 0.305 (95% CI 0.008–0.516), respectively. For the interobserver variability in the Altman–Bland plots, the mean differences were 11.5%, 2.6%, 1.3%, 12.6% and 15.2% of ADC_{min}, ADC_{mean}, ADC_{median}, $ADC_{97.5}$ and ADC_{max}, respectively.

Discussion

The presence of LN metastasis in cervical cancer patient is an independent and important prognostic factor [16, 17]. LN dissection remains the standard reference, but issues regarding the benefit of staging all cervical cancer and extent of assessment with potential postoperative complications still exist [18]. Recently, several promising techniques such as DWI or PET/CT have been used to detect LN metastasis in patients with cervical cancer, but diagnostic accuracy for detecting small normal-sized LN metastasis is still limited in clinical practice [6, 7]. Accordingly, a preoperative prediction model for assessing LN metastasis in cervical cancer

Table 1 Characteristics between cervical cancer patients with and without pelvic LN metastasis

	All patients ($n=162$)	LN metastasis (+) ($n=50$)	LN metastasis (−) ($n=112$)	p value
Age (years)	49.5 ± 11.6	48.6 ± 10.6	49.9 ± 12.0	0.510
FIGO				0.101
IA	3 (1.9)	0 (0.0)	3 (2.7)	
IB	114 (70.4)	31 (62.0)	83 (74.1)	
IIA	28 (17.3)	10 (20.0)	18 (16.1)	
IIB	17 (10.5)	9 (18.0)	8 (7.1)	
SCC antigen (ng/ml)	6.7 ± 12.8	10.0 ± 16.4	5.2 ± 10.6	0.009
Histology				0.407
SCC	116 (71.6)	38 (76.0)	78 (69.6)	
Adenocarcinoma/other	46 (28.4)	12 (24.0)	34 (30.4)	
Tumor size (cm)	3.5 ± 1.6	4.2 ± 1.4	3.3 ± 1.6	< 0.001
Long-axis LN (mm)	14.2 ± 3.9	15.7 ± 5.0	13.6 ± 3.1	0.005
Short-axis LN (mm)	9.1 ± 3.2	10.8 ± 4.5	8.4 ± 2.1	< 0.001
MRI T-stage, n (%)				< 0.001
T1A	2 (1.2)	0 (0.0)	2 (1.8)	
T1B	67 (41.4)	10 (20.0)	57 (50.9)	
T2A	30 (18.5)	11 (22.0)	19 (17.0)	
T2B	61 (37.7)	29 (58.0)	32 (28.6)	
T3	1 (0.6)	0 (0.0)	1 (0.9)	
T4A	1 (0.6)	0 (0.0)	1 (0.9)	
ADC histogram ($\times 10^{-3}$mm^2/s)				
$ADC_{97.5}$	1.271 ± 0.324	1.087 ± 0.171	1.354 ± 0.343	< 0.001
ADC_{mean}	0.969 ± 0.220	0.876 ± 0.120	1.010 ± 0.242	< 0.001
ADC_{median}	0.950 ± 0.224	0.872 ± 0.121	0.985 ± 0.250	0.004
ADC_{max}	1.340 ± 0.338	1.174 ± 0.244	1.414 ± 0.349	< 0.001
ADC_{min}	0.733 ± 0.201	0.676 ± 0.156	0.759 ± 0.215	0.016

Data are presented as mean ± standard deviation or n (%)

ADC apparent diffusion coefficient, *ADCn* nth percentile value of cumulative ADC histogram, *FIGO* International Federation of Gynecology and Obstetrics, *LN* lymph node, *SCC* squamous cell carcinoma

patients prior to surgery may allow for selection of optimal treatment strategies and improve patient counselling for prognosis.

DWI provides useful information for tumor aggressiveness, subtype characterization and treatment responses because of diffusion restriction in malignant tumors caused by increased cellular density [19]. Currently, this technique is widely used as a potential marker of tumor viability in oncologic imaging.

In this study, a predictive model using the ADC histogram was developed for assessing LN metastasis in patients with cervical cancer who underwent radical hysterectomy and pelvic LN dissection. Our results demonstrate that all ADC histogram variables in patients with pelvic LN metastasis had significantly lower ADC values than those without pelvic LN metastasis. On multivariate analysis, $ADC_{97.5}$ was the only independent predictor of pelvic LN metastasis. Furthermore, $ADC_{97.5}$ demonstrated the greatest AUC among the clinical and imaging variables at ROC curve analysis. These findings suggest that ADC histogram analysis might be a useful tool for predicting pelvic LN metastasis in cervical cancer patients who are scheduled for surgery. DWI can offer several advantages, such as noninvasive image acquisition, no requirement for contrast agents, and no exposure to ionizing radiation, and thus, is easily added to routine protocol for patient evaluation.

Several clinical risk factors for pelvic LN metastasis in patients with cervical cancer exist, such as tumor size, stage, age, depth of invasion, parametrial invasion, lymphovascular invasion, and SCC antigen [18, 20]. Our study included several clinical and imaging variables that could be obtained preoperatively. Tumor size, long-axis and short-axis diameter of pelvic LN, MRI T-stage and SCC antigen were significantly different between patients with and without pelvic LN metastasis. Moreover, all ADC variables demonstrated significantly lower ADC values in the group with LN metastasis than in the group without LN metastasis. This finding was consistent with a previous study [14]. An explanation

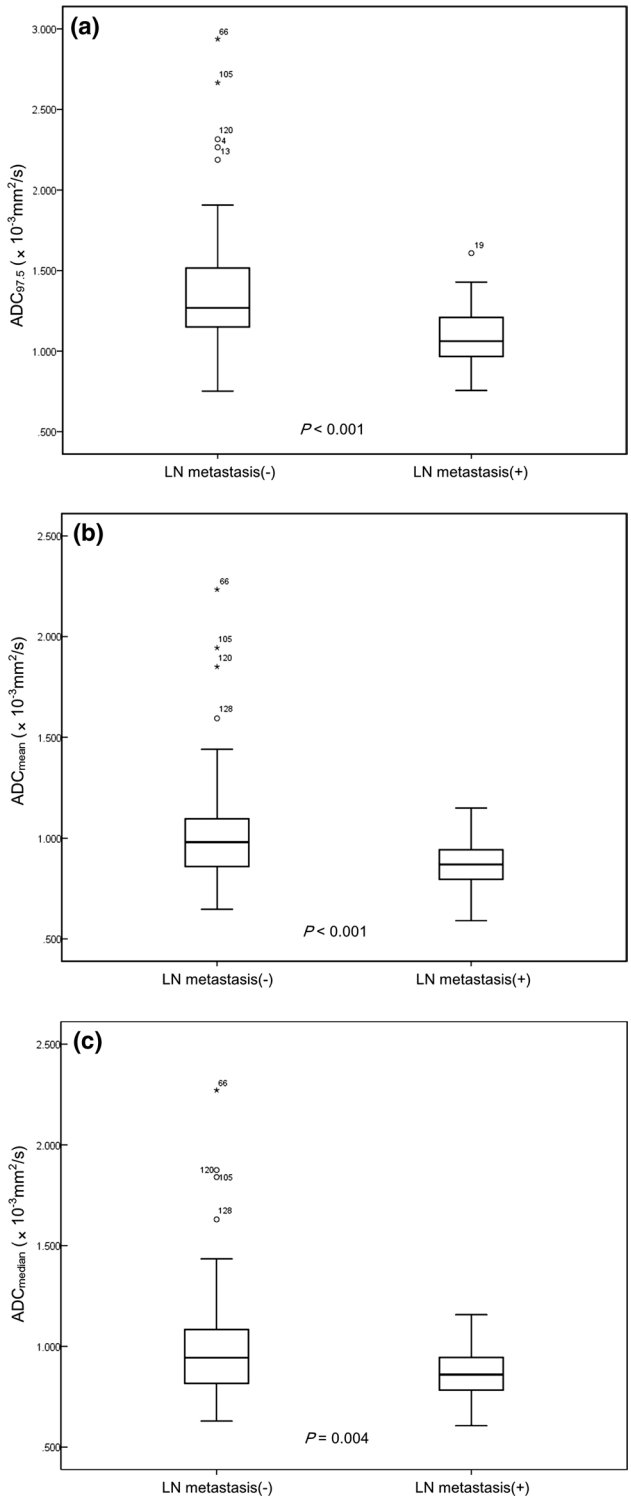

Fig. 3 Box-whisker plots demonstrate the values of $ADC_{97.5}$ (**a**), ADC_{mean} (**b**), ADC_{median} (**c**), ADC_{max} (**d**), and ADC_{min} (**e**) with and without pelvic LN metastasis. Central horizontal line = mean, and box = 25% and 75% confidence intervals

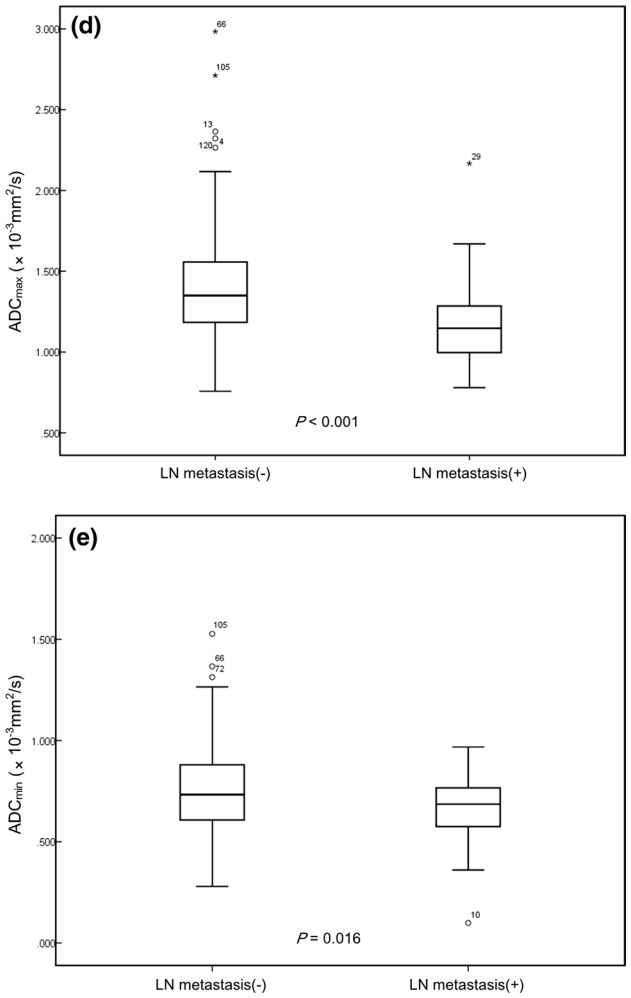

Fig. 3 (continued)

could be that poorly differentiated tumors have lower ADC values than well or moderately differentiated tumors [21], resulting in an increased likelihood of LN metastasis.

Univariate analysis demonstrated that long-axis and short-axis diameters of LN, MRI T-stage, SCC antigen, tumor size, and $ADC_{97.5}$ were significantly correlated with pelvic LN metastasis. However, only $ADC_{97.5}$ was a significant predictor of pelvic LN metastasis in the multivariate analysis. These findings suggested that the ADC97.5 might be used as a risk factor for pelvic LN metastasis in cervical cancer. However, further studies with internal or external validation will be needed.

For preoperative detection of LN metastasis in cervical cancer, a size criterion of MRI has been used with a threshold diameter of 10 mm in the short axis [5, 6]. However, this criterion is inaccurate because it overlaps sizes between metastatic, hyperplastic and normal LNs. Moreover, micrometastasis in small LNs is not rare. Morphologic features such as loss of normal LN architecture, irregular border,

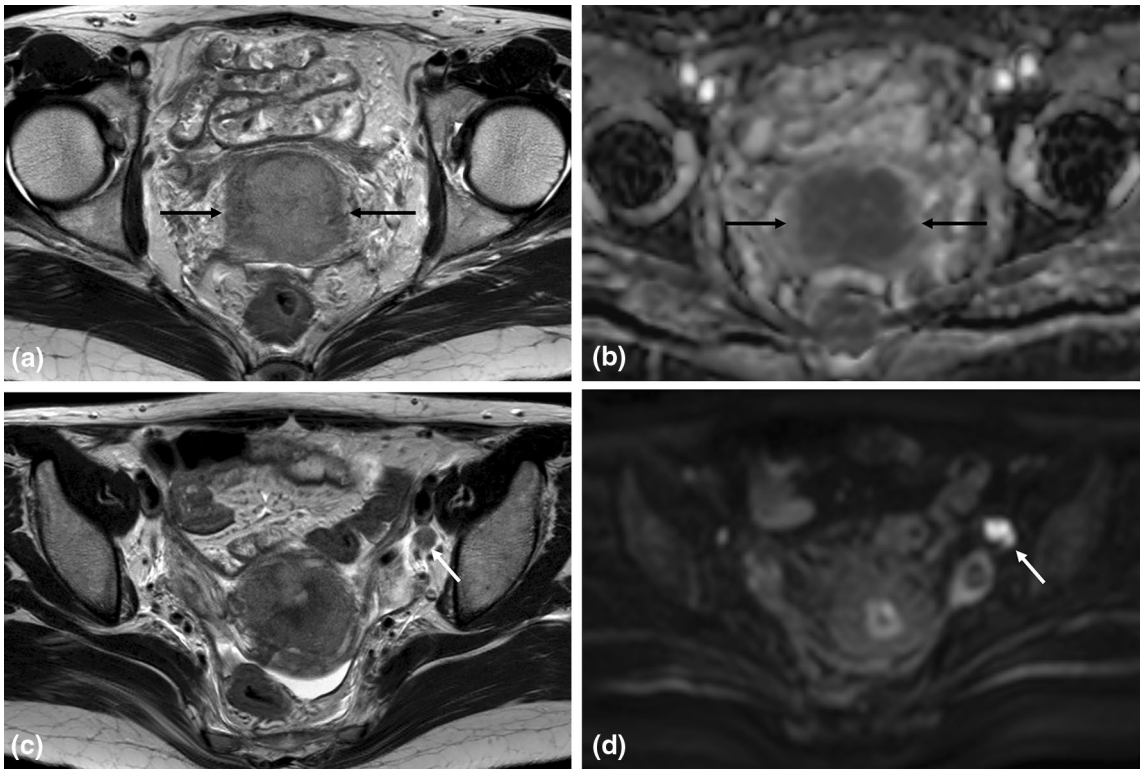

Fig. 4 A 42-year-old woman with FIGO stage IIB cervical cancer. **a**, **b** Axial T2-weighted image (**a**) shows a 5 cm cervical mass of high signal intensity, with bilateral parametrial invasion (arrows). On axial ADC map (**b**), the mass shows homogenous low signal intensity (arrows). On histogram analysis, ADC_{min}, ADC_{mean}, ADC_{median}, $ADC_{97.5}$, and ADC_{max} of the mass were 0.92, 1.023, 1.024, 1.130, and $1.151 \times 10^{-3} mm^2/s$, respectively. **c**, **d** Axial T2-weighted (**c**) and diffusion-weighted (**d**) images show an enlarged lymph node (arrow) of 15.2 × 12.3 mm in left internal iliac chain, suggesting a possibility of metastasis. Surgical specimen revealed no lymph node metastasis in the pelvis

rounder form, and heterogeneous signals are also used, but the diagnostic performance of MRI is limited to 67–95% accuracy, 37–90% sensitivity, and 71–100% specificity [6, 7]. Our study demonstrated that AUC, sensitivity, and specificity of $ADC_{97.5}$ were 0.782, 60%, and 83%, respectively. These values were the highest among all variables for predicting pelvic LN metastasis, followed by the short-axis LN diameter (0.704 AUC, 54% sensitivity, and 77% specificity). These results were consistent with previous studies [5–7].

An ADC map derived from DWI is commonly analyzed using the placement of the ROI in the tumor. However, this approach does not reflect the heterogeneity of whole tumors or the complex micro-architectural properties of malignantly transformed tissue. These limitations may be overcome with a histogram analysis using every voxel of the tumor [22, 23]. The histogram analysis can provide statistical information and a quantitative methodology for analyzing nonsignificant changes in the pixels of tumors. The percentiles may be useful in evaluating malignant components of lesions through the identification of different microenvironments that may be masked by mean ADC values. Only a few studies have used this histogram analysis of ADC maps for cervical cancer [2, 8, 14, 24]. Histogram analysis of ADC can distinguish normal cervical tissue from cervical cancer [2], and can separate well or moderately differentiated from poorly differentiated cervical cancer [8]. The predictive value of ADC-derived histogram variables for tumor recurrence in cervical cancer patients treated with chemoradiotherapy was reported [24]. Recently, Schob et al. [14] demonstrated significant differences in ADC-derived histogram variables comparing negative LN and positive LN in 18 cervical cancer patients. Consistent with this study [14], our results also showed that all ADC histogram variables were significantly lower in patients with LN metastasis than in those without LN metastasis. Currently, the histogram analysis of ADC is not available in all institutions. If the histogram analysis of ADC will be commercially available by MR vendors, it is expected that many researches will be performed for utility of ADC histogram analysis.

Reliability and variability are essential for assessing quantitative MRI variables as imaging biomarkers. Our results demonstrated that interobserver agreement for ADC_{min}, ADC_{mean}, and ADC_{median} was moderate to good, and that for ADC_{max} and $ADC_{97.5}$ were fair. And

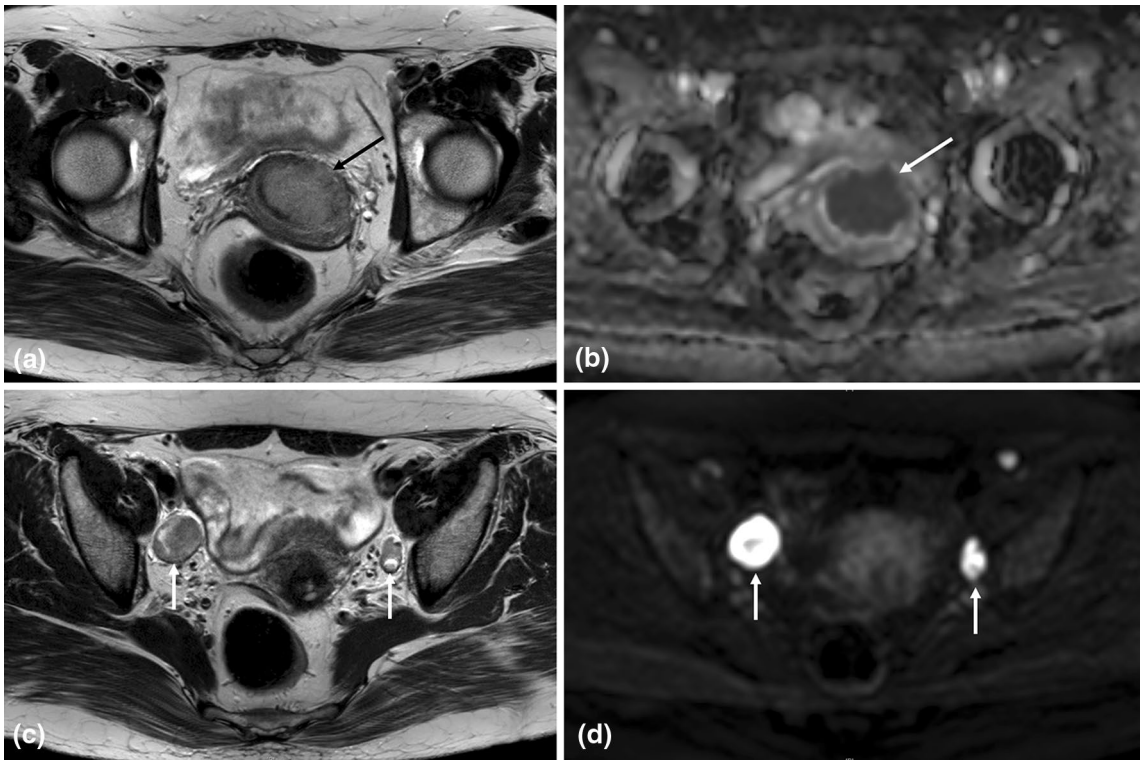

Fig. 5 A 53-year-old woman with FIGO stage IIB cervical cancer. Axial T2-weighted image (**a**) shows a 4.3 cm cervical mass of high signal intensity, with left parametrial invasion (arrow). On axial ADC map (**b**), the mass shows homogenous low signal intensity (arrow). On histogram analysis, A ADC_{min}, ADC_{mean}, ADC_{median}, $ADC_{97.5}$, and ADC_{max} of the mass were 0.671, 0.784, 0.778, 0.910, and $0.936 \times 10^{-3} mm^2/s$, respectively. Axial T2-weighted (**c**) and diffusion-weighted (**d**) images show two enlarged lymph nodes (arrows) in bilateral iliac chains suggesting a possibility of metastasis: right = 22.0 × 20.9 mm and left = 15.3 × 15.0 mm. Surgical specimen revealed lymph node metastasis in the bilateral internal iliac chains

Table 2 Logistic regression analysis for predicting pelvic LN metastasis

	Univariate			Multivariate		
	Odds ratio	95% Confidence interval	*p* value	Odds ratio	95% Confidence interval	*p* value
Age	0.990	0.962–1.020	0.508			
Long-axis LN	1.155	1.051–1.270	0.003	1.112	0.971–1.274	0.125
Short-axis LN	1.333	1.146–1.555	< 0.001	1.095	0.918–1.306	0.311
MRI T-stage (≥ T2B)	1.970	1.350–2.870	0.004	1.565	0.938–2.610	0.086
Histologic type	0.724	0.338–1.555	0.408			
FIGO stage (≥ IIB)	1.510	0.983–2.311	0.060			
SCC antigen	1.028	1.001–1.055	0.044	1.01	0.978–1.044	0.552
Tumor size	1.452	1.159–1.820	0.001	0.971	0.679–1.388	0.872
$ADC_{97.5}$	0.995	0.993–0.997	< 0.001	0.996	0.994–0.998	0.001

ADC apparent diffusion coefficient, $ADC_{97.5}$ 97.5th percentile value of cumulative ADC histogram, *CI* confidence interval, *FIGO* the International Federation of Gynecology and Obstetrics, *LN* lymph node, *OR* odds ratio, *SCC* squamous cell carcinoma

interobserver variability of ADC histogram ranged from 1.3 to 15.2%. Thus, ADC histogram variables might be used as imaging markers. However, to be commonly used in clinical practice, sophisticated software or standardized ROI measurement for tumors will be needed to improve reliability and reduce variability between observers.

There were several limitations in our study. First, our study was retrospective in a single center, with relatively small patient numbers. A further validation with a larger

Table 3 ROC curve analysis for predicting pelvic LN metastasis

Variables	AUC	Cutoff value	Sensitivity (%)	Specificity (%)
Age (year)	0.522 (0.428–0.616)	≤ 57	86	26
Long-axis LN	0.637 (0.545–0.729)	> 15.2	48	79
Short-axis LN	0.704 (0.614–0.793)	> 9.5	54	77
MRI T-stage	0.694 (0.614–0.773)	≥ T2B	80	53
Histologic type	0.532 (0.458–0.605)	SCC vs non-SCC	76	30
FIGO stage	0.594 (0.514–0.674)	≥ IIB	38	77
SCC antigen	0.634 (0.539–0.729)	> 1.7	62	62
Tumor size (cm)	0.667 (0.583–0.751)	> 3	84	51
$ADC_{97.5}$ ($\times 10^{-3}$mm^2/s)	0.782 (0.706–0.858)	≤ 1.092	60	83

ADC apparent diffusion coefficient, $ADC_{97.5}$ 97.5th percentile value of cumulative ADC histogram, *CI* confidence interval, *FIGO* the International Federation of Gynecology and Obstetrics, *LN* lymph node, *OR* odds ratio, *SCC* squamous cell carcinoma

numbers of patients will be needed to support clinical applications. Second, ADC values depend on many factors that cause changes in tissue diffusivity and regional gradients, such as body temperature, tissue pressure, perfusion rate, or an individual's magnetic environment [25]. To be used in clinical practice, DWI needs a standardized protocol across all institutions. This ideal is currently impossible. Third, the presence of paraaortic LN metastasis is an important prognostic factor [18], yet this aspect of cervical cancer was not analyzed in our study because of small number of patients in which LNs from the paraaortic region were dissected. Fourth, ADC values were not measured in the whole tumor in our study. Histogram analysis of ADC values in the whole tumor could evaluate more accurately tumor heterogeneity compared with a tumor showing the greatest dimension in a single image. However, the measurements in the whole tumor have still a potential limitation for mismatching between MRI and pathological findings. Fifth, we used perfusion-sensitive ADC values using b values of 0 and 1000 s/mm^2, which might overestimate the ADC values. To avoid contamination of the measured diffusion signal by capillary perfusion effects, adding of low b values of < 100–150 s/mm^2 will be needed in a future study [26].

In conclusion, our results show that $ADC_{97.5}$ from histogram analysis may be a useful marker for the prediction of pelvic LN metastasis in patients with cervical cancer. Preoperative ADC histogram analysis may be used to predict pelvic LN metastasis in patients with cervical cancer, which may play a crucial role for clinical decision making. However, a further study with a larger population is needed for validation.

Acknowledgements We thank Na Young Hwang MS and Insuk Sohn, Ph.D. of Statistics and Data Center, Samsung Medical Center, for help with statistical assistance.

Author contributions Study concepts and design: CKK, JL. Acquisition of data: CKK, JL, and SYP. Analysis and interpretation of data: CKK, JL, and SYP. Drafting of manuscript: CKK and JL. Critical revision: CKK, JL, and SYP.

Funding This study was funded by Basic Science Research Program through the National Research Foundation of Korea (NRF) funded by the Ministry of Education (NRF-2017R1A2B4006020).

Compliance with ethical standards

Conflict of interest All the authors (J.L., C.K.K., and S.Y.P.) declare that they have no conflict of interest.

Human participant and /or animals All the procedures performed in studies involving human participants were in accordance with the ethical standards of the institutional research committee and with the 1964 Helsinki Declaration and its later amendments or comparable ethical standards.

Informed consent Informed consent was obtained from all individual participants included in the study.

References

1. Torre LA, Islami F, Siegel RL, Ward EM, Jemal A (2017) Global cancer in women: burden and trends. Cancer Epidemiol Biomarkers Prev 26(4):444–457
2. Guan Y, Li W, Jiang Z, Chen Y, Liu S, He J, Zhou Z, Ge Y (2016) Whole-lesion apparent diffusion coefficient-based entropy-related parameters for characterizing cervical cancers: initial findings. Acad Radiol 23(12):1559–1567

3. Kupets R, Covens A (2001) Is the International Federation of Gynecology and Obstetrics staging system for cervical carcinoma able to predict survival in patients with cervical carcinoma? An assessment of clinimetric properties. Cancer 92(4):796–804
4. Bhatla N, Aoki D, Sharma DN, Sankaranarayanan R (2018) Cancer of the cervix uteri. Int J Gynaecol Obstet 143(Suppl 2):22–36
5. Choi HJ, Roh JW, Seo SS, Lee S, Kim JY, Kim SK, Kang KW, Lee JS, Jeong JY, Park SY (2006) Comparison of the accuracy of magnetic resonance imaging and positron emission tomography/computed tomography in the presurgical detection of lymph node metastases in patients with uterine cervical carcinoma: a prospective study. Cancer 106(4):914–922
6. Dappa E, Elger T, Hasenburg A, Duber C, Battista MJ, Hotker AM (2017) The value of advanced MRI techniques in the assessment of cervical cancer: a review. Insights Imaging 8(5):471–481
7. Liu B, Gao S, Li S (2017) A comprehensive comparison of CT, MRI, positron emission tomography or positron emission tomography/CT, and diffusion weighted imaging-MRI for detecting the lymph nodes metastases in patients with cervical cancer: a meta-analysis based on 67 studies. Gynecol Obstet Invest 82(3):209–222
8. Xue H, Ren C, Yang J, Sun Z, Li S, Jin Z, Shen K, Zhou W (2014) Histogram analysis of apparent diffusion coefficient for the assessment of local aggressiveness of cervical cancer. Arch Gynecol Obstet 290(2):341–348
9. Liu Y, Ye Z, Sun H, Bai R (2013) Grading of uterine cervical cancer by using the ADC difference value and its correlation with microvascular density and vascular endothelial growth factor. Eur Radiol 23(3):757–765
10. Park JJ, Kim CK, Park BK (2016) Prognostic value of diffusion-weighted magnetic resonance imaging and (18)F-fluorodeoxyglucose-positron emission tomography/computed tomography after concurrent chemoradiotherapy in uterine cervical cancer. Radiother Oncol 120(3):507–511
11. Park JJ, Kim CK, Park BK (2016) Prediction of disease progression following concurrent chemoradiotherapy for uterine cervical cancer: value of post-treatment diffusion-weighted imaging. Eur Radiol 26(9):3272–3279
12. Park JJ, Kim CK, Park SY, Simonetti AW, Kim E, Park BK, Huh SJ (2014) Assessment of early response to concurrent chemoradiotherapy in cervical cancer: value of diffusion-weighted and dynamic contrast-enhanced MR imaging. Magn Reson Imaging 32(8):993–1000
13. Onal C, Erbay G, Guler OC (2016) Treatment response evaluation using the mean apparent diffusion coefficient in cervical cancer patients treated with definitive chemoradiotherapy. J Magn Reson Imaging 44(4):1010–1019
14. Schob S, Meyer HJ, Pazaitis N, Schramm D, Bremicker K, Exner M, Hohn AK, Garnov N, Surov A (2017) ADC Histogram analysis of cervical cancer aids detecting lymphatic metastases—a preliminary study. Mol Imaging Biol 19(6):953–962
15. Pecorelli S (2009) Revised FIGO staging for carcinoma of the vulva, cervix, and endometrium. Int J Gynaecol Obstet 105(2):103–104
16. Takeda N, Sakuragi N, Takeda M, Okamoto K, Kuwabara M, Negishi H, Oikawa M, Yamamoto R, Yamada H, Fujimoto S (2002) Multivariate analysis of histopathologic prognostic factors for invasive cervical cancer treated with radical hysterectomy and systematic retroperitoneal lymphadenectomy. Acta Obstet Gynecol Scand 81(12):1144–1151
17. Morice P, Castaigne D, Pautier P, Rey A, Haie-Meder C, Leblanc M, Duvillard P (1999) Interest of pelvic and paraaortic lymphadenectomy in patients with stage IB and II cervical carcinoma. Gynecol Oncol 73(1):106–110
18. Gien LT, Covens A (2009) Lymph node assessment in cervical cancer: prognostic and therapeutic implications. J Surg Oncol 99(4):242–247
19. Hamstra DA, Rehemtulla A, Ross BD (2007) Diffusion magnetic resonance imaging: a biomarker for treatment response in oncology. J Clin Oncol 25(26):4104–4109
20. Takeshima N, Hirai Y, Katase K, Yano K, Yamauchi K, Hasumi K (1998) The value of squamous cell carcinoma antigen as a predictor of nodal metastasis in cervical cancer. Gynecol Oncol 68(3):263–266
21. Winfield JM, Orton MR, Collins DJ, Ind TE, Attygalle A, Hazell S, Morgan VA, deSouza NM (2017) Separation of type and grade in cervical tumours using non-mono-exponential models of diffusion-weighted MRI. Eur Radiol 27(2):627–636
22. Schob S, Meyer HJ, Dieckow J, Pervinder B, Pazaitis N, Hohn AK, Garnov N, Horvath-Rizea D, Hoffmann KT, Surov A (2017) Histogram analysis of diffusion weighted imaging at 3T is useful for prediction of lymphatic metastatic spread, proliferative activity, and cellularity in thyroid cancer. Int J Mol Sci 18(4):821
23. Just N (2014) Improving tumour heterogeneity MRI assessment with histograms. Br J Cancer 111(12):2205–2213
24. Heo SH, Shin SS, Kim JW, Lim HS, Jeong YY, Kang WD, Kim SM, Kang HK (2013) Pre-treatment diffusion-weighted MR imaging for predicting tumor recurrence in uterine cervical cancer treated with concurrent chemoradiation: value of histogram analysis of apparent diffusion coefficients. Korean J Radiol 14(4):616–625
25. Unger JB, Ivy JJ, Ramaswamy MR, Charrier A, Connor P (2005) Whole-body [18F]fluoro-2-deoxyglucose positron emission tomography scan staging prior to planned radical hysterectomy and pelvic lymphadenectomy. Int J Gynecol Cancer 15(6):1060–1064
26. Schob S, Meyer J, Gawlitza M, Frydrychowicz C, Muller W, Preuss M, Bure L, Quaschling U, Hoffmann KT, Surov A (2016) Diffusion-weighted MRI reflects proliferative activity in primary CNS lymphoma. PLoS ONE 11(8):e0161386